Static analysis and control strategies of the Single Active Bridge Converter

Alexis A. Gómez[1], Alberto Rodríguez[1], Marta M. Hernando[1], Diego G. Lamar[1], Javier Sebastián[1], Ibán Ayarzaguena[2], Jose Manuel Bermejo[2], Igor Larrazabal[2], David Ortega[2], Francisco Vázquez[3]

[1] Power Supply Systems Group. University of Oviedo, [2] Ingeteam Power Technology S.A., [3] Ingeteam R&D Europe.

[1] Gijón, Spain; [2] Zamudio, Spain; [3] Zamudio, Spain

E-Mail: gomezalexis@uniovi.es

URL: https://sea.grupos.uniovi.es/

Acknowledgements

Keywords

«DC-DC converter», «Isolated converter», «DC-DC power converter control», «Switching frequency control», «Single active bridge»

Abstract

In this paper, a brief static analysis of the Single Active Bridge, a unidirectional isolated DC-DC converter, is done. In this initial analysis the SAB is operating at a fixed frequency and controlled by varying the duty cycle. Additionally, two variable frequency control strategies are proposed that extends the soft-switching capabilities. This paper focuses on one of them that fixes the duty cycle and uses the switching frequency as the sole control variable. The conduction modes of the converter using the proposed control are analyzed and expressions for the voltage conversion ratio are obtained, which will be used in a design guide that provides ZVS over the full range of operation. A comparative current analysis is performed in which average, rms and switching currents of both control methods are depicted. Finally theoretical, simulation and experimental results are compared with good agreement.

Introduction

The Dual Active Bridge (DAB) is one of the reference converters when it comes to bidirectional and high-power density isolated DC-DC converters [1], [2]. In the case of applications where the power flows always in the same direction, it is possible to replace the secondary transistor bridge by a diode H-bridge; this substitution can potentially decrease the cost of the converter while improving its reliability and power density. The resulting converter has been called the Single Active Bridge (SAB), and several publications have examined the static behavior of this converter operating at a fixed frequency and controlled by varying the duty cycle [3]–[7].

Isolated DC-DC converters are subjects of development in different areas such as, battery chargers for electro mobility, renewable energies or second stages of grid tied converters. Several converter topologies are adequate for these applications, including the DAB and its variations. This document briefly introduces the static study of the SAB converter operating at a fixed frequency and controlled by varying the duty cycle and its conduction modes. Finally, two variable frequency control strategies are proposed, and one is analyzed. A design guide and simulation and experimental validation are provided. A general scheme of the SAB converter is shown in Fig. 1.
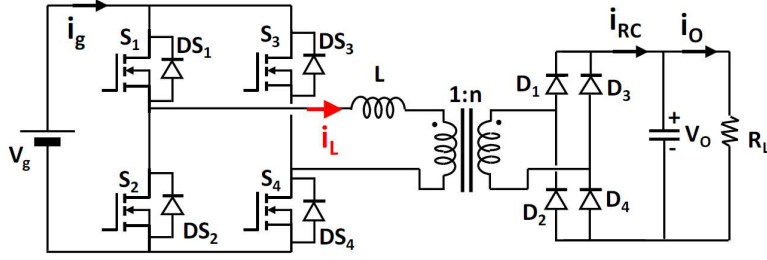
Fig. 1: Single Active Bridge (SAB) descriptive schematic.

Static analysis of the Single Active Bridge

A complete static analysis of the SAB operating at a fixed frequency and controlled by varying the duty cycle is presented in [6]. A brief explanation is introduced in this section, as a reference, to propose the variable switching frequency control, which is the main contribution of this paper.

The SAB can operate in two distinct conduction modes, Continuous Conduction Mode (CCM) and Discontinuous Conduction Modes (DCM). The operating mode of the converter is defined according to the current through the inductor L.

Continuous Conduction Mode (CCM)

This mode is characterized by an inductor current waveform that does not remain at zero, but only crosses zero on the transitions from the positive to the negative current stages and vice versa.

The analysis of the converter in this conduction mode starts by splitting a full switching period into 6 different stages and analyzing the current through the inductor (i_L) to find the voltage conversion ratio. This is done by averaging the transferred charge to the RC network over the full period. The i_L waveform for this mode is graphed in Fig. 2 and can be calculated by means of Faraday's Law.

Now analyzing each stage depicted in Fig. 2 a), from t_1 to t_2, S1 and S4 are closed, and the inductor withstands the input voltage minus the output voltage as seen from the primary side of the transformer, both voltages are supposed with negligible ripple. When the current reaches i_{L2} and from t_2 to t_3, S4 and DS2 conduct, the inductor withstands negative output voltage seen from the primary side. To finalize the positive current stages, from t_3 to t_4, DS2 and DS3 conduct and the voltage on the inductor is the negative sum of the input and output voltages, the latter as seen from the primary side. This analysis can be repeated in an analogue manner for the negative i_L stages.

Considering the current injected into the RC output network (i_{RC}), depicted in Fig. 2 b), it is possible to calculate the output voltage and the voltage conversion ratio for the SAB converter when working in CCM.

$$V_{o\_CCM} = R_L \, i_{RC\,average\,CCM} = \frac{R_L}{2\pi L T_s} \left[V_g t_c (T_s - t_c) - \frac{T_s^2 \left(\frac{V_o}{n}\right)^2}{4 V_g} \right] \tag{1}$$

$$N_{CCM} = \frac{V_o}{n \, V_g} = \frac{4 \, (1-d)d}{k + \sqrt{k^2 + 4 \, (1-d) \, d}} \tag{2}$$

$$t_c = t_2 - t_0 \tag{3}$$

$$d = \frac{t_c}{T_s} \tag{4}$$

$$k = \frac{2Ln^2}{R_L \frac{T_s}{2}} \tag{5}$$

Where, n is the transformer relation, d is the duty cycle, T_s is the switching period and, t_c is the time in which current flows through the input on a semi period, V_o and V_g are the output and input voltages, respectively. These equations show that the voltage conversion ratio when the converter operates in

CCM is heavily dependent on the connected load (R_L), contrary to other step-down converters when operating in this mode such as, the Buck or the Phase-Shifted Full Bridge (PSFB).

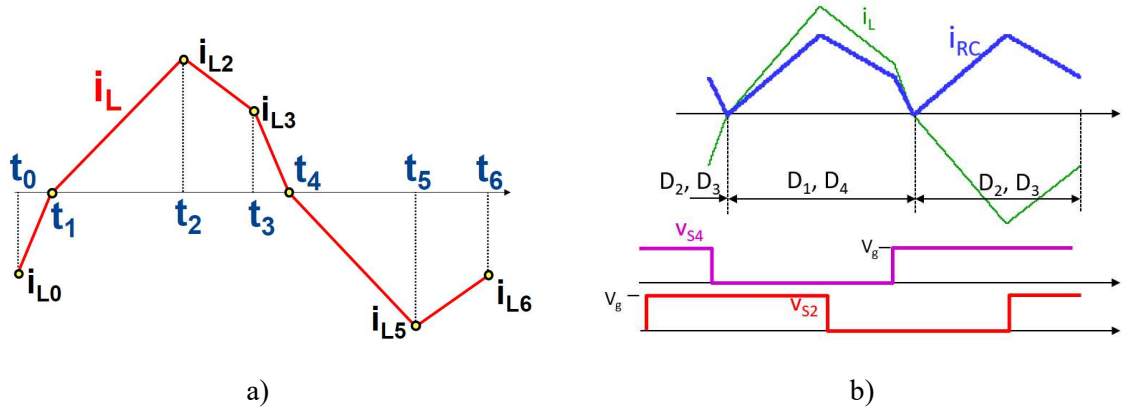a)   b)

Fig. 2: a) Inductor current in CCM. b) Inductor current and injected current to the RC network for CCM and voltage on the semiconductors.

Discontinuous Conduction Mode (DCM)

When the converter operates in DCM, the inductor and the RC network currents, graphed in Fig. 3, remains at zero from t_3 to t_4 and from t_0 to t_1, and no current flows through any semiconductor. The analysis methodology is analogue to that employed for CCM, resulting in:

$$V_{o\_DCM} = R_L \, i_{RC \, average \, DCM} = \frac{V_g \, R_L}{V_o L T_s} \left[V_g - \frac{V_o}{n} \right] t_c^2 \tag{6}$$

$$N_{DCM} = \frac{V_o}{n \, V_g} = \frac{2d}{d + \sqrt{d^2 + k}} \tag{7}$$

In this mode, the output voltage and the voltage conversion ratio depend again on the connected load, as for other step-down converters.

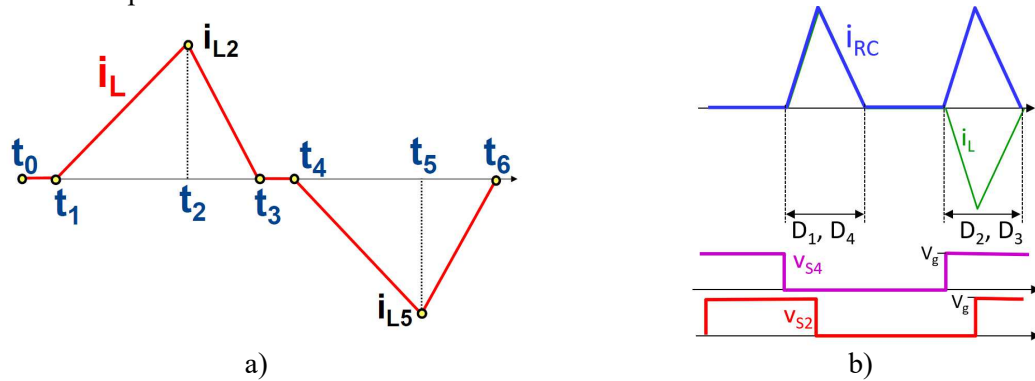a)   b)

Fig. 3: a) Inductor current in DCM. b) Inductor current and injected current to the RC network for DCM and voltage on the semiconductors.

Boundary between CCM and DCM

The converter operates in the boundary between both conduction modes when t_3 and t_4; t_0 and t_1 are the same instant, respectively; and the inductor current is zero. As in the boundary mode the converter does not operate strictly in neither conduction mode, both voltage conversion relations must be correct, therefore equations (2) and (7) must be valid for this operating point, resulting in:

$$k_{crit} = 1 - 2d_{crit} \tag{8}$$

$$k_{crit} = \frac{2Ln^2}{R_{L \, crit} \frac{T_s}{2}} \tag{9}$$

$$N_{crit} = \left(\frac{V_o}{n\,V_g}\right)_{crit} = 2d_{crit} \tag{10}$$

As with other similar converters, such as the Buck or the PSFB, the converter enters DCM from CCM when the connected load is greater than a specific value, function of the parameters of the converter and control variables values.

Variable frequency control

Up to this point the converter was considered operating at a fixed frequency and controlled by varying the duty cycle (d), as defined in (4). This strategy allows for a regulated output current or voltage by changing the duty cycle as a function of input voltages and power levels. As the switching period appears on the voltage conversion ratio equation for DCM and CCM, the switching frequency can also be used as a control variable. To maximize the range of operation, a duty cycle controlled SAB must operate in both CCM and DCM. On the one hand, the SAB converter while operating in CCM can achieve Zero Voltage Switching (ZVS) [8], [9]; however, when working in DCM this is not possible. On the other hand, conduction losses are generally higher for CCM than DCM, this is due to a greater semiconductor RMS current value, greater average currents, and the presence of excess recirculating currents, necessary for soft-switching.

To operate the SAB in CCM over a wide range while maintaining a minimum amount of recirculating current, the SAB can be controlled by varying the frequency. Two possible control possibilities arise from this additional control variable, a control with fixed duty cycle and a variable switching frequency; and a control strategy where both are variable. For both control methods, the main idea is to operate in CCM at any operating point, guaranteeing ZVS. For the first strategy the necessary recirculating current to achieve soft-switching must be guaranteed, therefore this level of current is stablished at the maximum operating frequency and minimum load; as the duty cycle is fixed, the recirculating current at greater power levels, lower operating frequencies, will be greater than necessary. If the second alternative is chosen, as there are two control variables, the recirculating currents can be kept at the minimum level over the entire range of operation, at the expense of an extended switching frequency range. This paper will focus on the first approach. Ideal current waveforms for both approaches are graphed in Fig. 4.
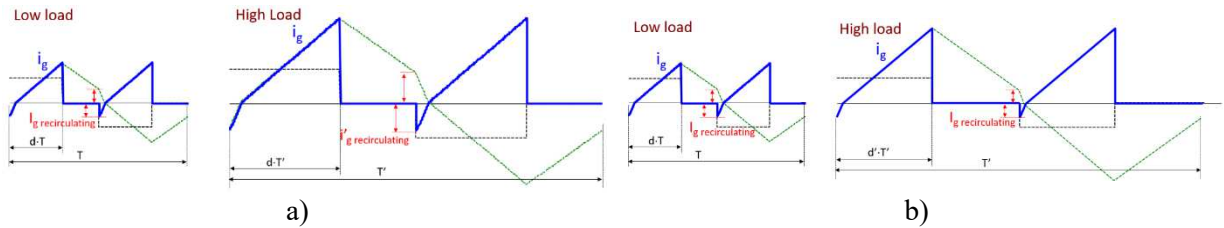

a)   b)

Fig. 4: Ideal inductor current waveforms with minimum recirculating current to achieve ZVS at different loads. a) Fixed duty cycle and variable switching frequency. b) Variable duty cycle and switching frequency.

Static analysis for variable frequency

By observing (2) and (7), if the duty cycle remains constant, to maintain a constant voltage conversion ratio the product $T\,R_L$ must remain constant, this implies a linear relation between the switching frequency and the connected load. Reformulating (2) and (7), the linear relation previously mentioned is clearly appreciated in the following equations.

$$f_{CCM} = \left(\frac{(1-d)d}{2N} - \frac{N}{8}\right)\frac{R_L}{n^2 L} \tag{11}$$

$$f_{DCM} = \frac{(1-N)d^2}{N^2}\frac{R_L}{Ln^2} \tag{12}$$

In Fig. 5 a) and b) the "open loop" behavior of the converter is shown, understood as the converter response to a fixed control variable as a function of the connected load and for different duty cycles and switching frequencies. In Fig. 5 c) and d) the "closed loop" behavior is depicted, understood as the control variable value required to obtain a specific response; this is done again as a function of load and for several duty cycles and normalized voltage conversion ratios. Fig. 5 and (10) show that the boundary between conduction modes is set by the value of the duty cycle, therefore if it is greater than half of the normalized voltage conversion ratio, CCM operation is guaranteed over all the operating range.
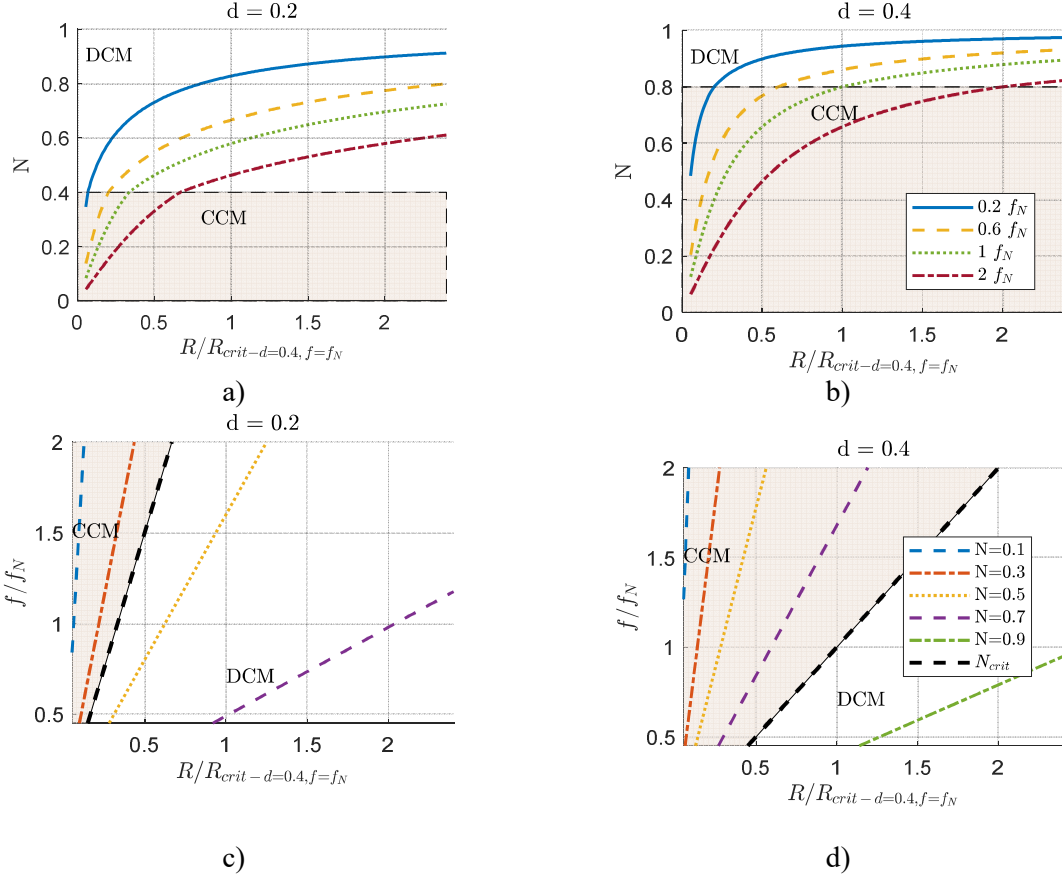

Fig. 5: a) and b) Normalized voltage conversion ratio (N) as a function of normalized load, for different switching frequencies. c) and d) Normalized switching frequency as a function of normalized load, for different values of N.

For the current analysis, input and recirculating average currents are compared for variable duty cycle and variable frequency control strategies. Input and output voltages are supposed ripple free, and all converter components are considered ideal. For both conduction modes, the average input current is described by:

$$\overline{I_g} = 2/T \left[\int_{t_1}^{t_2} i_g(t) \ dt + \int_{t_0}^{t_1} i_g(t) \ dt \right] \tag{13}$$

It can be appreciated in (13) that current only flows through the input in two intervals (from t_1 to t_2 and from t_0 to t_1). The current on the first interval is positive and appears on both conduction modes, the second interval is characterized by a negative current in CCM and null in DCM, this is the recirculating current. Equations (14) and (15) express the average input current for CCM and DCM respectively. To obtain the average recirculating current expression (18), an analogue method is followed.

$$\overline{I_{g\ CCM}} = \frac{1}{TL}\left[\left(V_g - \frac{V_o}{n} \right)(t_2 - t_1)^2_{MCC} - \left(V_g + \frac{V_o}{n} \right)(t_1 - t_0)^2_{CCM} \right] \tag{14}$$

$$\overline{I_{g\,DCM}} = \frac{1}{TL}\left[\left(V_g - \frac{V_o}{n}\right)(t_2 - t_1)_{DCM}^2\right] \tag{15}$$

$$(t_2 - t_1)_{CCM} = \frac{T}{2}\left(d + \frac{V_o}{2V_g n}\right) \tag{16}$$

$$(t_2 - t_1)_{DCM} = dT \tag{17}$$

$$\overline{I_{recirculating}} = \frac{1}{TL}\left(V_g + \frac{V_o}{n}\right)(t_1 - t_0)_{CCM}^2 \tag{18}$$

$$(t_1 - t_0)_{CCM} = \frac{T}{2}\left(d - \frac{V_o}{2V_g n}\right) \tag{19}$$

By relating (18) and (14) equation (20) is obtained. It shows that the relation of average recirculating current to the average input current is independent of the switching frequency; and only depends on the converter design, input and output voltages and duty cycle.

$$\frac{\overline{I_{recirculating}}}{\overline{I_{g\,CCM}}} = \frac{\left(V_g + \frac{V_o}{n}\right)\left(d + \frac{V_o}{2nV_g}\right)^2}{\left(V_g - \frac{V_o}{n}\right)\left(d - \frac{V_o}{2nV_g}\right)^2 - \left(V_g + \frac{V_o}{n}\right)\left(d + \frac{V_o}{2nV_g}\right)^2} \tag{20}$$

Design guide

This design process aims to design a SAB converter that operates in CCM for all operating points, therefore achieving ZVS. With this purpose, the maximum critical duty cycle (d_{crit}) is set, and this value will serve as the inferior limit of the available duty cycle range (21). The initial specifications necessary for the design process are:

- Input and output voltage ranges.
- Output current range.
- Switching frequency range.

As mentioned, the first step is to set an adequate maximum critical duty cycle. The actual duty cycle should be superior to this value; the closer they both are, the less recirculating current.

$$d_{crit} \leq d \leq 0.5 \tag{21}$$

The duty cycle is used in (22) to find the transformation relation of the transformer. Once calculated, the inductor value that achieves the minimum voltage conversion ratio (23) at the maximum frequency specified is obtained. This is the minimum value of L. By doing this with (24), the minimum power operating point is fixed at the top of the specified frequency range. Finally, the minimum frequency is checked to be within the specified frequency range with (26).

$$n_{min} = \frac{V_{o\,max}}{2d_{crit}V_{g\,min}} \tag{22}$$

$$N_{min} = \frac{V_{o\,min}}{n\,V_{g\,max}} \tag{23}$$

$$L = \left(\frac{(1-d)d}{2N_{min}} - \frac{N_{min}}{8}\right)\frac{\frac{V_{o\,min}}{I_{o\,min}}}{n^2 f_{max}} \tag{24}$$

$$N_{max} = \frac{V_{o\,max}}{n\,V_{g\,min}} \tag{25}$$

$$f_{min} = \left(\frac{(1-d)d}{2N_{max}} - \frac{N_{max}}{8}\right)\frac{\frac{V_{o\,max}}{I_{o\,max}}}{n^2 L} \tag{26}$$

Alternatively, the operating point to fix during the design process can be the one corresponding to the minimum frequency; to achieve this, an analogue process should be followed. In this occasion, the L value calculated corresponds to the maximum, and it is necessary to check the maximum frequency to be below the specified maximum. This is done by using expressions (27) and (28).

$$L = \left(\frac{(1-d)d}{2N_{max}} - \frac{N_{max}}{8}\right)\frac{\frac{V_{o\,max}}{I_{o\,max}}}{n^2 f_{min}} \tag{27}$$

$$f_{max} = \left(\frac{(1-d)d}{2N_{min}} - \frac{N_{min}}{8}\right)\frac{\frac{V_{o\,min}}{I_{o\,min}}}{n^2 L} \tag{28}$$

A comparative design example between this design guide and the one exposed in [6] is done with the following specifications:
- Input voltage range: [800 V, 850 V].
- Output voltage range: [350 V, 400 V].
- Output current range: [0.5 A, 5.5 A].
- Acceptable switching frequency range: [22 kHz, 300 kHz].

The picked maximum critical duty (d_{crit}) cycle for both design guides is 0.25, and the variable frequency design has a fixed duty cycle of 0.275. The results of both design procedures are in Table I. Control variable values are graphed in Fig. 6 as a function of the output current for different input and output voltages. Fig. 6 a) corresponds to the design of variable duty cycle and can be appreciated that the converter operates in both conduction modes; whereas Fig. 6 b), corresponds to the variable frequency design and only operates in CCM, as this was one of the criteria used for the design guide. The switching frequency of the first design is 33 kHz.
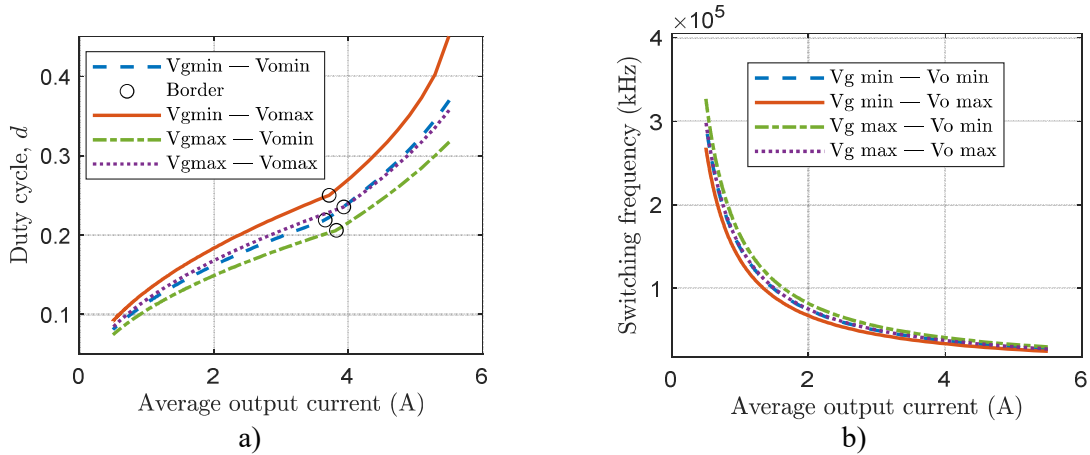

Fig. 6: Control variable values as a function of the average output current for different input and output voltages. a) Converter controlled by a variable duty cycle. b) Converter controlled by a variable switching frequency.

Table I: Resulting designs.

Design	Transformer relation (n)	Inductor value (L)
Variable duty cycle	1	408 μH
Variable switching frequency	1	444 μH

Current through the semiconductors

To compare both designs, rms and average current though the semiconductors have been calculated (these values provide a comparison of conduction losses). All currents are calculated for minimum input and maximum output voltages.

Fig. 7 a) shows the rms currents through a pair of semiconductors on the input side as a function of the average output current. With equal transformer relations, in general the variable frequency design operates with lower levels of rms current, due to a better inductor current waveform. Because of the design guide criteria, the variable frequency converter suffers the presence of a small recirculating current at all operating points that increases proportionally with the average output current, as predicted by (20). On the contrary, the variable duty cycle design only has recirculating current at CCM operating points.
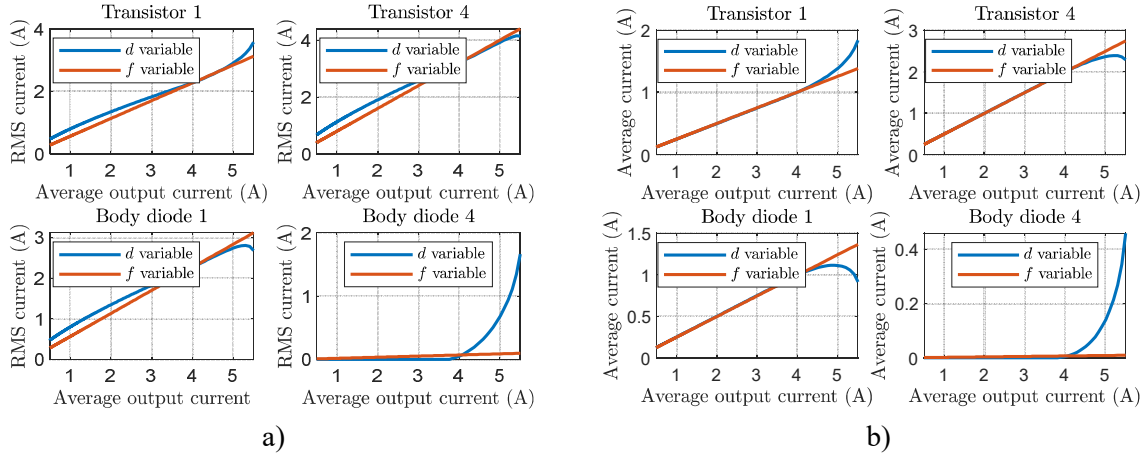

Fig. 7: Semiconductor currents for both designs. a) RMS currents. b) Average currents.

For the average currents, represented in Fig. 7 b), in the regions where the variable duty cycle design operates in DCM, the average currents are similar, this changes once both alternatives operate in CCM. Finally, Fig. 9 shows the inductor's current, i_L, at the switching events, this is of interest to compare switching losses. All the simulations were done using the software PSIM considering all components ideal; accurate correlation between analytical predictions and simulation results were obtained.

Experimental results

In this section experimental results of a duty cycle controlled SAB and a switching frequency controlled SAB are provided. The prototype used for the experimental validation was designed with the design guide of [6] resulting in the specifications of Table . The inductor is integrated in the leakage inductance of the transformer. With this prototype all previous equations are validated, and results are provided for both control strategies. The input and output voltages for all tests are 800 V and 400 V, respectively.

Table II: Experimental prototype specifications.

Transformer relation (n)	Inductor value (L)
1	408 µH

Equations (14), (15), (18) and (20) are graphed in Fig. 8. Fig. 8 a) and c) correspond to a converter controlled by a variable duty cycle and designed with the design guide from [6]. Fig. 8 b) and d) correspond to a converter designed to be controlled by a variable frequency. Fig. 8 a) and b) represent the average input current as a function of the control variable. Fig. 8 c) and d) represent the average normalized recirculating current as a function of the control variable for each converter design. From Fig. 8 it is possible to understand that high duty cycles result in a higher power transfer, but more relative recirculating current, which increases conduction losses. For this reason, to maximize the use of the converter the duty cycle must remain high, so the transferred power is high without reaching for excessively low switching frequencies; at the same time if the preferred operating mode is CCM, the maximum critical duty cycle should be high as well to minimize the recirculating current. Fig. 8 d) shows a relative recirculating current constant over the complete range, which results in excess recirculating current at higher power levels than the minimum.
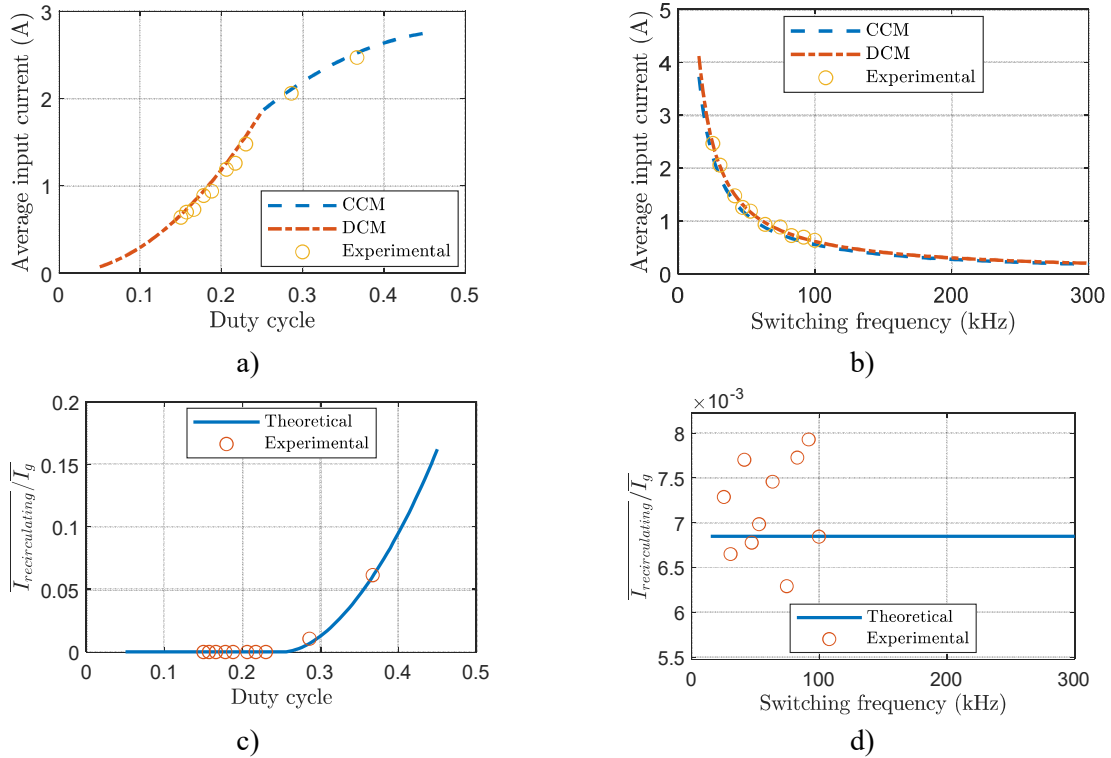
Fig. 8: a) and b) Average input current as a function of the control variable; duty cycle and switching frequency, respectively. c) and d) Relation of average recirculating and input currents as a function of the control variable; duty cycle and switching frequency, respectively.
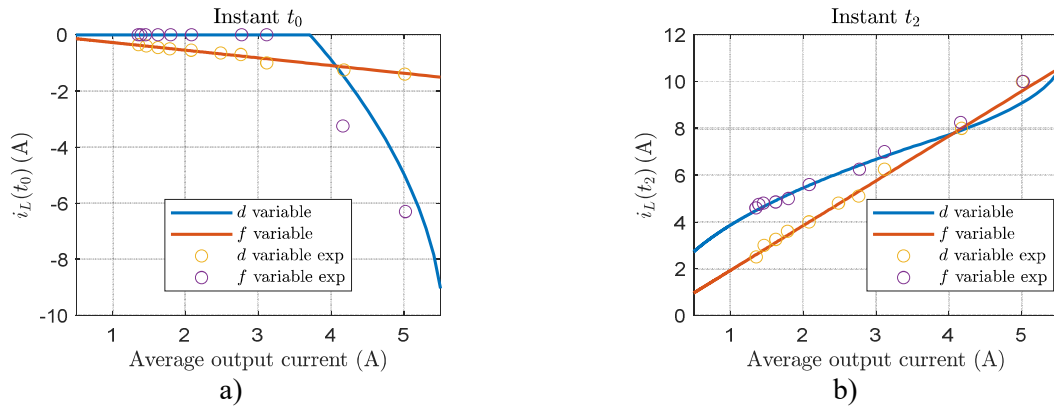

Fig. 9: Inductor current at the switching instants; theoretical and experimental, for both designs.

Fig. 10 a) Shows the theoretical, simulated, and experimental value of the switching frequency for the fixed duty cycle design when the input and output voltages are minimum and maximum respectively. Fig. 10 b) and c) are oscilloscopes captures when the converter operates at 91 % and 29 % of the nominal load. Yellow and green [5 V/div] are gate signals corresponding to channels 1 and 2 respectively; purple [5 A/div] is channel 3 and measures the inductor's current; magenta [200 V/div] is the drain voltage of one of the switches. [10 µs/div].
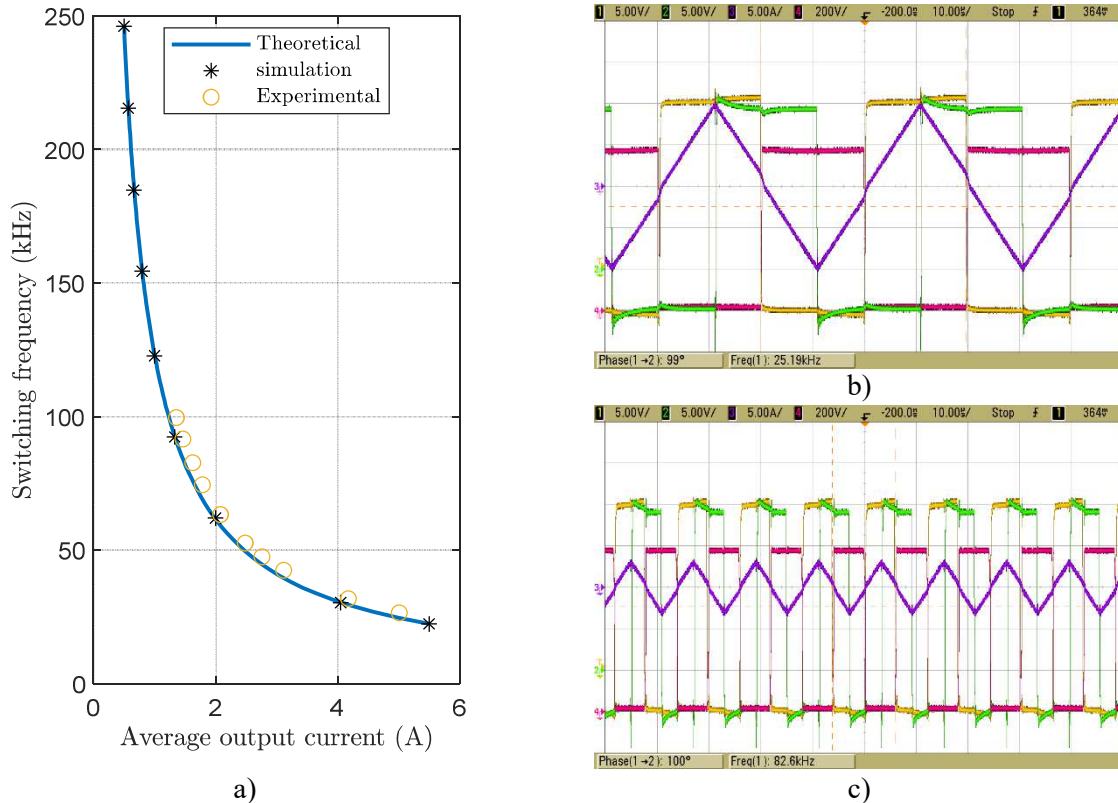
Fig. 10: a) Switching frequency as a function of the average output current; theoretical, simulated, and experimental results. b) and c) Oscilloscope captures of two operating points.

Finally, an efficiency comparison between the two control methods is done and graphed in Fig. 11. In this figure the efficiency of both control strategies as a function of the average output current is shown. In general, the proposed control strategy yields better efficiency, specially at high loads. Only at lower power levels the variable duty cycle achieves better performance, due in part to the absent recirculating currents.
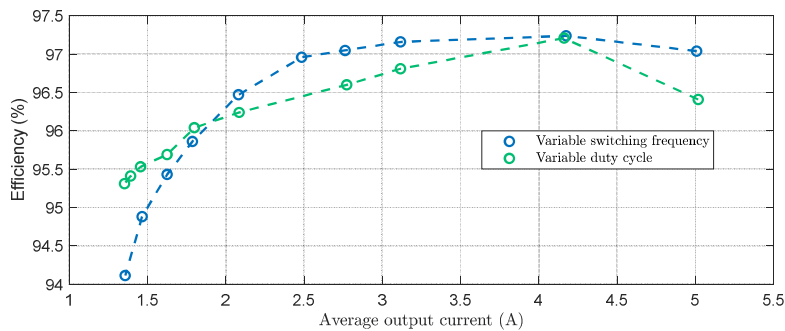

Fig. 11: Efficiency comparison.

Conclusion

A brief static analysis of the SAB converter is done, it shows a directly proportional relation between the switching frequency and the connected load, in CCM and DCM. Recirculating current proportion to average input current is independent of switching frequency, which makes a variable frequency control adequate to maintain ZVS over a wider range than a duty cycle based control. Due to the linearity between load and frequency, the frequency range can be excessively high, which makes for difficult and decreased performance magnetic design. From the current analysis, conduction losses seem similar in both cases, and efficiency is in general slightly improved except at low power. A control strategy with both, the switching frequency and the duty cycle, as control variables could reduce the excessive frequency range.

References

[1] A. R. Rodríguez Alonso, J. Sebastian, D. G. Lamar, M. M. Hernando, and A. Vazquez, "An overall study of a Dual Active Bridge for bidirectional DC/DC conversion," in *2010 IEEE Energy Conversion Congress and Exposition*, Sep. 2010, pp. 1129–1135. doi: 10.1109/ECCE.2010.5617847.

[2] A. Rodríguez, A. Vázquez, D. G. Lamar, M. M. Hernando, and J. Sebastián, "Different Purpose Design Strategies and Techniques to Improve the Performance of a Dual Active Bridge With Phase-Shift Control," *IEEE Transactions on Power Electronics*, vol. 30, no. 2, pp. 790–804, Feb. 2015, doi: 10.1109/TPEL.2014.2309853.

[3] C. Fontana, M. Forato, M. Bertoluzzo, and G. Buja, "Design characteristics of SAB and DAB converters," in *2015 Intl Aegean Conference on Electrical Machines & Power Electronics (ACEMP), 2015 Intl Conference on Optimization of Electrical & Electronic Equipment (OPTIM) & 2015 Intl Symposium on Advanced Electromechanical Motion Systems (ELECTROMOTION)*, Side, Turkey, Sep. 2015, pp. 661–668. doi: 10.1109/OPTIM.2015.7427025.

[4] A. Averberg and A. Mertens, "Characteristics of the single active bridge converter with voltage doubler," in *2008 13th International Power Electronics and Motion Control Conference*, Poznan, Poland, Sep. 2008, pp. 213–220. doi: 10.1109/EPEPEMC.2008.4635269.

[5] G. D. Demetriades, "On small-signal analysis and control of the single- and dual-active bridge topologies," Stockholm, 2005.

[6] A. Rodriguez *et al.*, "An Overall Analysis of the Static Characteristics of the Single Active Bridge Converter," *Electronics*, vol. 11, no. 4, Art. no. 4, Jan. 2022, doi: 10.3390/electronics11040601.

[7] C. A. Tuan, H. Naoki, and T. Takeshita, "Unidirectional Isolated High-Frequency-Link DC-DC Converter Using Soft-Switching Technique," in *2019 IEEE 4th International Future Energy Electronics Conference (IFEEC)*, Singapore, Singapore, Nov. 2019, pp. 1–7. doi: 10.1109/IFEEC47410.2019.9015117.

[8] G. D. Demetriades and H. P. Nee, "Characterisation of the Soft-switched Single-Active Bridge Topology Employing a Novel Control Scheme for High-power DC-DC Applications," in *IEEE 36th Conference on Power Electronics Specialists, 2005.*, Aachen, Germany, 2005, pp. 1947–1951. doi: 10.1109/PESC.2005.1581898.

[9] C. Fontana, M. Forato, K. Kumar, M. T. Outeiro, M. Bertoluzzo, and G. Buja, "Soft-switching capabilities of SAB vs. DAB converters," in *IECON 2015 - 41st Annual Conference of the IEEE Industrial Electronics Society*, Yokohama, Nov. 2015, pp. 003485–003490. doi: 10.1109/IECON.2015.7392640.